Volume 7, Issue 2, 2026

Trends in
Natural Products Research

Green Synthesis of Hydroxyapatite Nanoparticles from Catfish Bone: A Novel Approach for Sustainable Biomaterial intended for Biomedical Applications.

Frank Ohwoavworhua*, Abishag Stephen, Ademola Oduola, Mamuda Bappah

Department Of Pharmaceutics and Pharmaceutical Technology, Faculty of Pharmaceutical Sciences, Gombe State University, Gombe State.

Abstract

The objective of this study was to develop a green synthetic method of production of hydroxyapatite (HAp) nanoparticles from catfish bone, considered as an excellent source due to its abundance and low cost. Hydroxyapatite is a highly versatile biomaterial, and its significance in biomedical science has led to investigation into its numerous synthetic methods, which include: precipitation, hydrothermal, biomimetic deposition, electrodeposition, calcination and alkaline hydrolysis techniques. Most of these techniques have limitations ranging from the use of 'cocktail' of inorganic and organic compounds – making the process very expensive, the risk of agglomerations, the high-energy requirement, to the risk of formation of a second phase reaction. We report a novel method of synthesizing hydroxyapatite nanoparticles from catfish bones using 20 % sodium hydroxide solution at 80 °C under vigorous stirring. The hydroxyapatite nanomaterial was characterized for the elemental compositions, the chemical groups present using the Fourier transform infrared spectroscopy (FTIR), the crystallite nature using the X-ray diffraction (XRD), the morphology using the scanning electron microscopy (SEM), and the thermal profile using the thermogravimetric analysis (TGA), as well as the powder properties determinations. The results showed HAp nanoparticles exhibited irregular shapes rather than a specific particle shape; the elemental analysis revealed the existence of calcium and phosphate ions as oxides, as well the presence of some trace elements that will benefit tissue engineering. The powder properties indicate that HAp nanomaterial have fair to passable flow properties, while the moisture sorption capacity indicates that the material is capable of taking up water if not properly stored. The findings suggest that the hydroxyapatite nanoparticles derived from catfish bone have particulate and powder properties suitable for pharmaceutical and biomedical applications.

Keywords: Catfish bone, Hydroxyapatite nanoparticles, Alkaline hydrolysis, Characterization.

*Corresponding author:
frankohwo@gsu.edu
+2348037738358
https://doi.org/10.61594/tnpr.v7i2.2026.161
Page No.: 121-129
Volume: Volume 7 Issue 2, 2026
Trends in Natural Products Research
Copy Right: NAPREG

Received 5/3/26, Revised 14/3/26, Accepted 19/3/26, Published 21/4/2026

Introduction

Hydroxyapatite (HAp), as a remarkable biomaterial, finds applications in medicine and biomedicine. For instance, it is used to make dental filling because of its excellent biocompatibility; for mammalian bone regeneration (osteoclast and osteoblast cells), bioimaging, cancer therapy, and drug delivery (Okpe *et al.,* 2024). HAp has also found use in catalysis when it combines with other metals and metal oxides (Ofudje *et al.,* 2019). In these uses, the nanomeric materials are more reactive and have better physicochemical qualities due to significantly larger exposed surface area (Okpe *et al*., 2024) HAp is the main inorganic component of human bone. Its similarity to natural bone mineral makes it an ideal material for bone grafts and implants (Zhou *et al*., 2011). HAp from natural sources contains ions such as Na^{+}, Zn^{2+}, Mg^{2+}, K+, Si^{2+}, Ba^{2+}, F^{-} and CO_3^{2-} (Novivanti *et al*., 2020). HAp can be synthesized from chemical sources however; it is complicated and biologically unsafe. (Okpe *et al* 2024). The chemical synthesis involves the use of precursors, such as calcium and phosphorous, as well as phosphoric acid (H_3PO_4) and calcium hydroxide ($Ca(OH)_2$.

The many applications of hydroxyapatite nanoparticles in biomedical and pharmaceutical industries have led to various scientific efforts in its synthesis, and many approaches have been reported including precipitation-, hydrothermal-, biomimetic deposition-, electrodeposition-, calcination-, and alkaline hydrolysis techniques (Okpe *et al.,* 2024). These techniques, however, have limitations. For example, the precipitation method has the risk of agglomeration formation, as well as requires the use of 'cocktails' inorganic and organic compounds - making the process very expensive (Bouyer *et al.,* 2000). The hydrothermal and calcination methods utilize high-energy input because temperatures range of 750 ^{0}C – 1400 ^{0}C is required (Okpe *et al.,* 2024). Also, the risk of formation of secondary phase reaction limits the substitution techniques (Ofudje *et al.,* 2019; Okpe *et al.,* 2024), while high-energy requirement, though not as high as calcination, requiring temperature set up as high as 250 ^{0}C to 750 ^{0}C (Barakat *et al.,* 2009; Sun *et al.,* 2017). The alkaline synthetic method is considered most economical and facile, and hence investigations into this method of production of hydroxyapatite nanoparticles continue to be progressive (Ofudje *et al*., 2019; Okpe *et al*., 2024).

It is against this background that this project seeks to obtain HA nanoparticles from the catfish bone using the 'alkaline synthetic' method at a very low temperature of 80 ^{0}C with vigorous stirring. This method is therefore innovative because of very low energy consumption, since the alkaline hydrolysis of catfish bone was achieved at 80 ^{0}C with vigorous stirring – hence it is "Green".

The aim of this study was to investigate a facile novel method for production and characterization of hydroxyapatite nanoparticles from alkaline hydrolysis at a very low temperature.

Materials and Method

Materials

The materials used in this were distilled water, mortar and pestle, sodium hydroxide, beakers, spatula, glass rod, magnetic stirrer, hot plate, Buchner funnel, filter paper, analytical weighing balance, hot air oven, measuring cylinder, crucible, acetone, retort stand, ruler, thermometer, scanning electron microscope and thermogravimetric analysis machine.

Collection of Fish Bone

The catfish, *Clarias gariepinus,* was bought in Gombe main market. It was identified in the Department of Biological Sciences, Faculty of Science, Gombe State University. The flesh was stripped from the bones and the bones were thoroughly washed with hot water to remove the flesh. The bones were dried in an oven at 50 ^{0}C for 8 h.

Preparation of sample

The catfish bones were crushed in a mortar and the powder was suspended in to 700 mL of 20 % sodium hydroxide solution under vigorous magnetic stirring. Stirring was continued for 6 h, and the resultant slurry was washed with distilled water and then filtered under vacuum using Buchner funnel. The resulting residue was washed thrice and dried. The residue was pulverized in a mortar to obtain hydroxyapatite nanoparticles, which was then characterized using the following techniques.

Scanning Electron Microscopy (SEM)

The SEM was used to examine the morphological characteristics of the HAp sample. The sample was placed on double adhesive, which was on a sample stub, and sputter coated with 5 nm of gold. Thereafter, it was placed into the chamber of SEM machine where it was viewed via NaVCaM for focusing, and adjustment before it was transferred to SEM mode. The brightness and contrast were automatically adjusted and the image obtained.

X-Ray Powder Diffractometer (XRD) Studies

To assess the crystalline or amorphous nature of samples, XRD at ambient temperature was used. The powder sample, packed in rectangular aluminum cell, was illuminated using CuKα radiation (λ=1.54056 Å) at 45 kV and 40 mA. The sample was scanned between diffraction angles of 0° to 70° 2θ, which is sufficient to cover all significant diffraction peaks of HAp crystallites. Scan steps of 0.1 with a dwell time of 15s were used. A nickel filter was used to reduce the Kβ contribution to the X-ray signal (Manek *et al.,* 2012).

Fourier Transform Infrared (FTIR) Spectroscopy

Fourier transform infrared (FTIR) spectroscopic technique was used to determine the functional groups present in the HAp sample. Few milligrams of the sample were mixed with KBr, compressed into pellet following standard operating procedures and this was scanned at range 4500 to 500 cm^{-1} (Manek *et al.,* 2012).

Thermogravimetric Analysis

Thermogravimetric analysis was conducted on a TGA machine. The runs were conducted from temperature range of 30^0 to 950^0 C at a heating rate of 10^0C min^{-1}, under nitrogen atmosphere at 60 mL min^{-1} and the balance contained 20 mg of the sample (Clara *et al.,* 2018).

Elemental Analysis

The HAp sample was weighed into 32 mm sample cups with a polypropylene X-ray film of 4 µm thickness and was hydraulically pressed. Sample heights were measured in mm and sample cups were capped. The EDXRF analysis was performed using a Rigaku NEX EDXRF spectrometer equipped with a fifteen-place sample changer with spin function using slow and steady spinning mode (Ofudje *et al.,* 2019).

Powder properties characterizations

Solubility tests

The hydroxyapatite nanoparticle (1 g) was weighed and added to 10ml of distilled water. It was mixed thoroughly and left at room temperature for 30min. The mixture was centrifuged at 2500 rpm for 10 min. The supernatant was collected and evaporated to dryness in at 80 ^{0}C. The procedure was repeated using 0.1 N HCL, and 75 % methanol (USP-NF, 2020).

True density

This was determined by the specific gravity bottle method (Ohwoavworhua and Okhamafe, 2020). A 50 mL specific gravity bottle was filled with acetone (a) and its weight determined. About half of the acetone was discarded and 2 g of the sample (w) was transferred into the bottle; more acetone was added to the bottle until it was filled up and its weight was again determined (b). The true density (Dt) was calculated using the Equation below.

$$Dt = w/ [(a + w) – b] \times SG$$

Bulk and Tapped densities

The powder sample (20 g) was transferred into a 50 mL measuring cylinder and the volume (V_0), occupied without tapping was determined. After 500 taps, the volume (V_{500}) was determined. The bulk, and tapped densities were calculated as the ratio of weight to volume (V_o and V_{500} respectively).

Bulk- or tapped density = weight of powder (g) / volume of powder (mL)

Angle of repose

The static angle of repose *a*, was measured according to the fixed funnel and free standing cone method (Train *et al.,* 1958). A glass funnel, secured with a plug, was mounted on a retort stand at a height of 2 cm above a graph paper placed on a flat horizontal surface. The sample (20 g) was carefully transferred into the funnel and the plug was removed to allow the sample to flow until it successfully formed a heap on the graph paper (with a height, *h*). The mean diameter (D), of the base of the powder cone was determined and the tangent of the angle of repose calculated thus.

$$\text{Tan } a = 2h/D$$

Moisture content

The sample (2 g) was weighed and transferred into a clean, dry evaporating dish and then dried at 80 ^{0}C to a constant weight. The percent loss in weight was calculated as the moisture content of the sample.

Moisture sorption capacity

The sample (1 g) was weighed and evenly distributed inside a 90 mm Petri dish. It was then placed in a desiccator containing distilled water in its reservoir. The desiccator was then covered and left at room temperature. The sample was weighed daily over a period of 5 days and the weight gained by the sample was recorded. The moisture adsorbed was calculated from the weight difference.

Results

The yield of HAp nanoparticles derived from the catfish bones using 20 % W/V sodium hydroxide at 80 °C with vigorous stirring was 99.7 % (n = 2).

Scanning Electron Microscopy (SEM)

The scanning electron micrograph, (SEM), revealed that Aloe vera hydrocolloid consists of particles of colloidal dimensions, ranging from few nanometers to micrometers

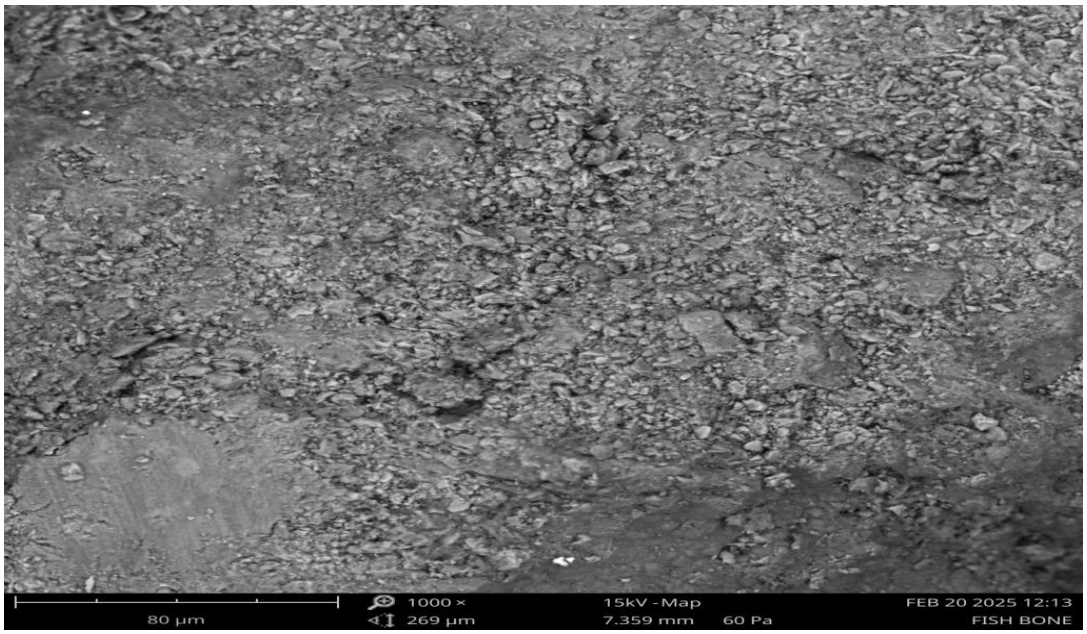

Figure 1: SEM of the hydroxyapatite nanoparticles (x 1000).

X-Ray Powder Diffractometer (XRD) Studies

The X-ray diffraction pattern of the HAp nanomaterial indicated the HAp nanomaterial is highly crystalline. This crystalline form exhibits a principal peak around 35 2θ. The figure represents a classic pattern of a crystalline substance (Figure 2).

Fourier Transformed Infra-red (FTIR) Spectroscopy

The FTIR spectrum of the HAp nanoparticles showed medium peaks between 1416.38838cm^{-1} and 879.65cm^{-1}, indicating asymmetric stretching due to CO_3^{2-}. The peak at 1021.29057cm^{-1} corresponds to PO_4^{3-}. The peaks such as 3537.94cm^{-1} and 2922.2cm^{-1} are very weak small and almost rudimentary (Figure 3).

Thermogravimetric Analysis (TGA)

The HAp thermogram can be divided into three main stages of weight loss and that HAp could withstand temperature rise up to approximately 250 ^{0}C. The thermal properties of the hydroxyapatite nanomaterial occurred as thermograms, namely: the TGA curve (broken line curve) and the derivative thermograph (DTG, boldline curve) (Figure 4).

The DTG curve showed an optimum decomposition temperature (OPT) of the HAp material at 340 °C. Furthermore, the DTG curve showed a thermal decomposition temperature range of about 300 °C (that is from 200 to 500 °C).

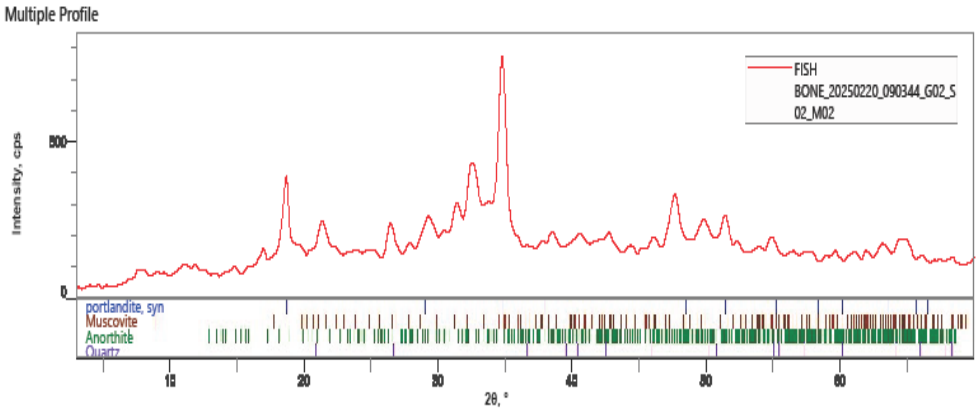

Figure 2: XRD **diffractogram of the hydroxyapatite nanoparticles**

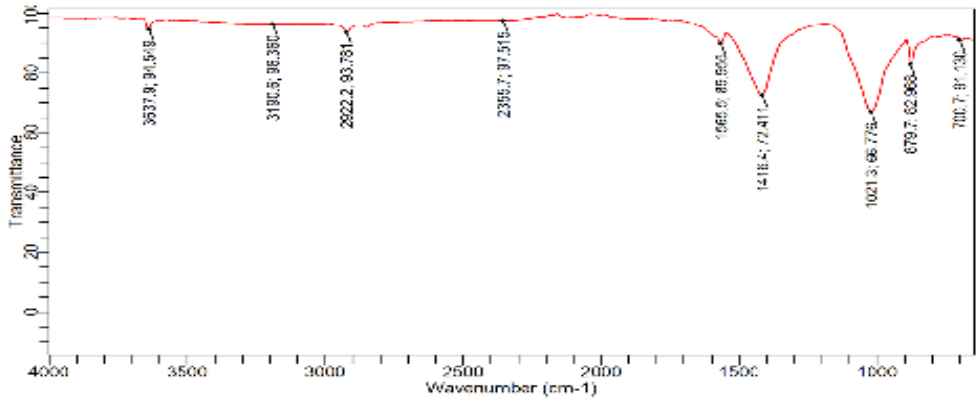

Figure 3: FTIR spectrum of the hydroxyapatite nanoparticles

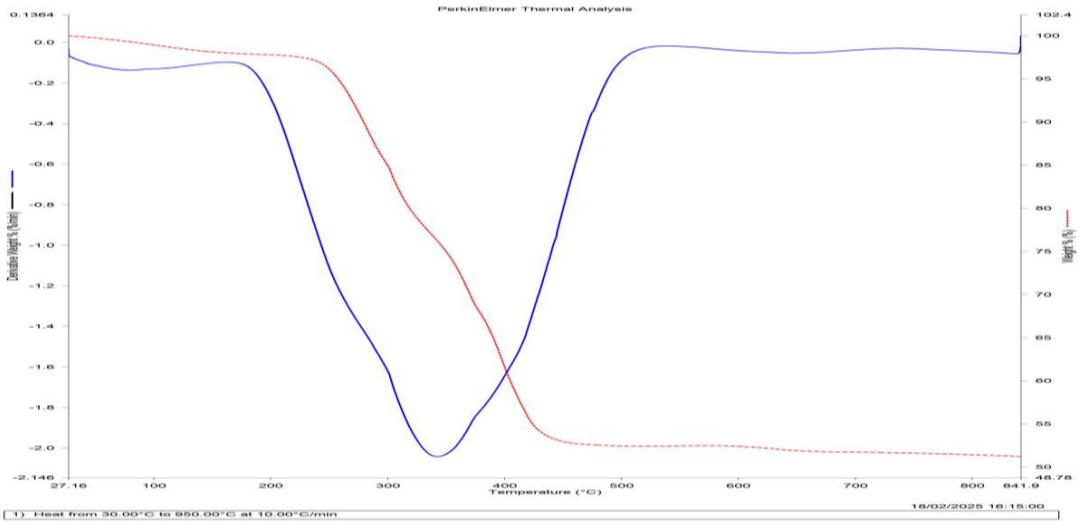

Figure 4: TGA thermogram of the hydroxyapatite nanoparticles

Elemental and Oxides Composition Analysis

Tables' 1a and 1b present the results of the elemental and oxides compositions of HAp sample as analyzed using the EDXRF. The S, CL, Sr were found to be present in significant amount. Transition metals; Ni, Cu, Zn, and Zr and alkaline earth metals; Ba and Sr were also found to be present in appreciable quantity. The halogen, Br was found to be present in minor quantity. The oxides of phosphorous and calcium showed high values of 22.9 and 60 %, respectively (Table 1b).

Powder properties characterization

Table 2 presents the powder properties of the hydroxyapatite nanoparticles and showing its physical characteristics and potential processing behavior. The results revealed the bulk density (1.1216 g/cm³) and tapped density (1.4425 g/cm³), and the angle of repose is 35.86 °. The solubility of hydroxyapatite nanoparticles in distilled water, 0.1N HCL, and methanol was 33.3%, 64.8322%, and 7.41% respectively, while the moisture adsorption capacity at the end of day 5 is 20.8362%.

Table 1a: Elemental composition of the hydroxyapatite nanoparticles

Component	Result (ppm)
S	1690
CL	1330
Ni	53.2
Cu	83.4
Zn	119
Br	9.76
Sr	938
Zr	88.2
Ba	58.3

Table 1b: Oxides composition of the hydroxyapatite nanoparticles

Component	Result (mass%)
Na_2O	15.1
Al_2O_3	0.449
SiO_2	0.604
P_2O_5	22.9
CaO	60.0
MnO_2	0.0332
Fe_2O_3	0.0698

Table 2: Properties of fish bone-derived hydroxyapatite nanoparticles

Parameters	Results
Bulk density	1.1216
Tapped density	1.4425
Angle of repose (°)	35.8633
True density	1.2954
Solubility:	
a. In water	33.3%
b. In 0.1N HCl	64.8233%
c. In methanol	7.41%
Moisture content	2.218%
Moisture Sorption Capacity	20.84%

Discussion

The high yield of HAp indicates that catfish bones are composed predominantly of hydroxyapatite nanomaterial.

The rough and porous surface characteristics as revealed by the SEM are considered advantageous for biomedical applications as it could enhance cell attachment and proliferation (Zhou and Lee 2011). The observed morphology is consistent with previous studies on biologically derived hydroxyapatite nanoparticles; particularly those obtained from natural sources such as fish bones (Venkatesan *et al*., 2015).

The X-ray diffraction technique is a non-destructive analytical technique that provided detailed information about the internal arrangement of the crystalline substances (Castillo et al., 2018). Although, there are other peaks of lower intensity around 18, 33, and 47 2θ, the presence of a principal peak around 35 2θ suggests its crystalline form. The result obtained is similar to that of Rama (2023) and Okpe *et al.,* (2024).

Fourier transform infrared spectroscopy has been utilized more extensively in the present day to keep track of the chemical make-up and functional groups (Mandal *et al.,* 2006). Ojo *et al.,* (2022) reported that the peaks at 3537.94cm^{-1} and 2922.2cm^{-1} are associated with the bending vibration of hydroxyl group of HAp and those at peaks between 1416.38838cm^{-1} and 879.65cm^{-1}, suggest asymmetric stretching due to CO_3^{2-} and the peak at 1021.29057cm^{-1} corresponds to PO_4^{3-}.

The TGA analysis measures the change in mass of a sample as a function of temperature. The analysis provides information about the moisture content and decomposition mechanism of a sample, and the thermal transitions of a material, where a mass loss occurs with each thermal event, which implies the volatilization of one or more components (Castillo *et al*., 2018). Tõnsuaadu *et al*., (2012) explained that the first stage, the drying stage, occurring below 250 °C, is attributed to the loss of adsorbed water; the second stage, the pyrolytic stage, occurs between 250 and 450 °C, represents the decomposition of residual organic matter that may have remained after the alkaline hydrolysis process; and the third stage, the decarboxylation stage, observed above 450 °C, could be associated with the loss of structural water and partial decomposition of carbonate species present in the HAp structure The thermal profile beyond 650 °C to 841 °C, where the residual weight is fairly constant (no significant loss in weight), could be attributed to inorganic element content of HAp. On the other hand, the DTG curve (bold line plot) showed a 2 % weight loss, which is in tandem with moisture content of 2 % determined by weight loss method in the hot air oven. The DTG curve showed the HAp nanomaterial has only one endothermal

peak, which indicates that the decomposition is under single stage degradation. The thermal profile is important as it can enable the formulation scientist to predict how well pharmaceutical formulations involving the HAp can withstand high temperatures.

For the elemental and oxides analysis, Akram *et al.,* (2014) reported that the presence of beneficial cations such as Ni^{2+}, Cu^{2+}, Sr^{2+}, Ba^{2+}, Zr^{4+} and anion Br^{-} could be consider to play important roles in tissue engineering and other biochemical reactions.

The bulk density and tapped density values are within the range typically reported for hydroxyapatite powders (Ramesh *et al*., 2013). The values indicate moderate compactness of the powder, which is important for processing applications such as compaction of pharmaceutical powder.

The angle of repose value indicates that HAp powder had fair to passable flow properties according to the USP classification (USP <1174>) This moderate flowability could be attributed to the nanoscale dimensions and surface characteristics of the particles, which increase interparticle forces and reduce flowability compared to larger particles. For pharmaceutical applications, this may necessitate the use of flow aids or granulation processes to improve processability.

The high solubility of HAp nanoparticles in 0.1N HCL shows that it will be an excellent excipient for pharmaceutical formulations, particularly oral delivery dosage forms. Moisture content plays an important role in the stability of pharmaceutical formulations. High moisture content favors bacterial growth and chemical degradation. The result of moisture content of less than 3% is considered appropriate for pharmaceutical formulations, whose moisture content ranges from 3-7 %.

Moisture sorption capacity plays a critical role in the stability of pharmaceutical formulations. High moisture adsorption capacity of a sample will favor instability in moisture sensitive formulations, and the moisture adsorption capacity suggests that the sample should be kept in airtight container to avoid moisture adsorption.

Conclusion

Hydroxyapatite nanoparticle has been successfully synthesized from catfish bones using alkaline hydrolysis method - 20% NaOH solution at 80 °C with continuous vigorous stirring, with 99.7 % yield. The results from the various characterizations – particulate and powder properties, suggest that hydroxyapatite nanoparticles derived from catfish bones would be suitable for pharmaceutical and biomedical applications.

References

Akram M, Ahmed R, Shakir et al (2014). Extracting hydroxyapatite and its precursors from natural resources. *Journal Material Science* 49:1461-1475.

Barakat NA, Khil MS, Omran A, Sheikh FA, Kim HY (2009). Extraction of pure natural hydroxyapatite from the bovine bones bio waste by three different methods. *Journal of Materials Processing Technology* 209(7): 34083415.

Bouyer E, Gitzhofer F, Boulos MI (2000). Morphological study of hydroxyapatite nanocrystals suspension. *Journal of Material Science: Materials in Medicine* 11(8): 523-531.

Castillo L., German M R., Rolando V Z., Gustavo C. (2018). Combined use of DSC, TGA, XRD and NIR in the Compatibility study of preformulation mixtures for the development of 10 mg tablets of Rupatadine Fumarate. *Journal of Drug Delivery and Therapeutics* 8(3): 42-54

Manek VR, Philip FB, William MK et al (2012). Physicochemical and binder properties of starch obtained from *Cyperus esculentus*. *American Association of Pharmaceutical Scientist* 13(2): 379- 388.

Noviyanti AR, Akbar N, Deawati Y et al (2020). A novel hydrothermal synthesis of nanohydroxyapatite from egg shell-calcium oxide precursors. *Heliyon* 6: e03655.

Ofudje EA, Adeogun AI, Idowu MA, Kareem SO (2019). Synthesis and characterization of Zn-doped hydroxyapatite: scaffold application, antibacterial and bioactivity studies. *Heliyon* 5(5): e01716.

Okpe PC, Folorunso O, Aigbodion VS, Obayi C (2024). Hydroxyapatite synthesis and characterization from waste animal bones and natural sources for biomedical applications. *Journal Biomedical Material Research* 112(7): e35440.

Ojo OE, Sekunowo OI, Ilomuanya MO et al (2022). Structural and morphological evaluations of natural hydroxyapatite from calcined animal bones for biomedical applications. *Journal of Casting and Material Engineering* 6(1): 14-21.

Ohwoavworhua FO, Ogah E, Kunle OO. (2005). Preliminary investigation of physicochemical and functional properties of alpha cellulose obtained from waste paper- A potential pharmaceutical excipient. *Journal of Raw Materials Research* 2(2): 84-93.

Poinern GEJ, Brundavanam RK, Mondinos N, Jiang ZT (2009). Synthesis and characterisation of nanohydroxyapatite using an ultrasound assisted method. *Ultrasonics Sonochemistry* 16(4): 469-474.

Rama Talat Rashad (2023). Simple extraction of the hydroxyapatite from the Egyptian Nile tilapia (*Oreochromis niloticas*) fish scales. *Acta Scientifica Malaysia* 7(2): 60-65.

Ramesh S, Tan CY, Sopyan I et al (2013). Consolidation of nanocrystalline hydroxyapatite powder. *Science and Technology of Advanced Materials* 8(2), 124-130.

Sun RX, Lv Y, Niu YR, et al (2017). Physicochemical and biological properties of bovine-derived porous hydroxyapatite/collagen composite and its hydroxyapatite powders. *Ceramic International Journal* 43(18): 16792-16798.

Tõnsuaadu K, Gross KA, Plūduma L, Veiderma M (2012). A review on the thermal stability of calcium apatites. *Journal of Thermal Analysis and Calorimetry* 110(2): 647-659.

Train D (1958). Some aspects of the property of angle of repose of powders. *Journal of Pharmacy and Pharmacology* 10: 127T-134T.

Venkatesan J, Qian ZJ, Ryu B et al (2015). Preparation and characterization of carbon nanotube-grafted-chitosan—Natural hydroxyapatite composite for bone tissue engineering. *Carbohydrate Polymers* 83(2): 569-577.

Zhou H, Lee J (2011). Nanoscale hydroxyapatite particles for bone tissue engineering. *Acta Biomaterialia* 7(7): 2769-2781.

This paper is published under Creative Common Licence BY 4.0

CITATION: Ohwoavworhua F, Stephen A, Oduola A, Bappah M (2026) Green Synthesis of Hydroxyapatite Nanoparticles from Catfish Bone: A Novel Approach for Sustainable Biomaterial intended for Biomedical Applications.
Trend Nat Prod Res Vol 7(2): 121-129. https://doi.org/10.61594/tnpr.v7i2.2026.161